Experimental Mechanics (2011) 51:833–843
DOI 10.1007/s11340-010-9394-7

Bayesian Statistic Based Multivariate Gaussian Process Approach for Offline/Online Fatigue Crack Growth Prediction

S. Mohanty · A. Chattopadhyay · P. Peralta · S. Das

Received: 30 October 2009 / Accepted: 18 July 2010 / Published online: 27 August 2010

Abstract Offline and online fatigue crack growth prediction of Aluminum 2024 compact-tension (CT) specimens under variable loading has been modeled, using multivariate Gaussian Process (GP) technique. The GP model is a Bayesian statistic stochastic model that projects the input space to an output space by probabilistically inferring the underlying nonlinear function. For the offline prediction, the input space of the model is trained with parameters that affect fatigue crack growth, such as the number of fatigue cycles, minimum load, maximum load, and load ratio. For the online prediction, the model input space is trained using piezoelectric sensor signal features rather than training the input space with loading parameters, which are difficult to measure in a real time scenario. Principal Component Analysis (PCA) is used to extract the principal features from sensor signals. In both the offline and online case, the output space is trained with known associated crack lengths or crack growth rates. Once the GP model is trained, a new output space for which the corresponding crack length or crack growth rate is not known, is predicted using the trained GP model. The models are validated through several numerical examples.

S. Mohanty (✉) · A. Chattopadhyay · P. Peralta
Arizona State University,
Tempe, AZ 85287, USA
e-mail: subhasish.mohanty@asu.edu

A. Chattopadhyay
e-mail: aditi@asu.edu

P. Peralta
e-mail: pperalta@asu.edu

S. Das
NASA Ames Research Center,
Moffett Field, CA 94035, USA
e-mail: Santanu.Das-1@nasa.gov

Keywords Fatigue life prediction · Statistical method · Structural health monitoring · Probabilistic approach · Variable loading · Gaussian process

Nomenclature

a_i	i^{th} random crack length
$\widehat{a}_{N+1}$	$\text{N}+1^{\text{th}}$ mean prediction
D	$\{\mathbf{x}_i, a_i\}_{i=1}^{N}$ Gaussian Process training space
d	Input dimension
M	Number of sensor observation at any fatigue instance
N	Number of different fatigue cycle (instances)
$\mathbf{K}_N$	$N \times N$ kernel matrix for Gaussian Process input-output space mapping
$\mathbf{x}_i$	$1 \times d$ i^{th} Fatigue instances input vector
$\mathbf{a}_N$	$N \times 1$ training or known output vector
Θ	Gaussian process hyperparameters
$\mathbf{C}_d$	$d \times d$ covariance matrix for PCA feature extraction
$\mathbf{y}_d$	$1 \times d$ Sensor observation

Introduction

Aircraft maintenance must balance labor, logistics, and equipment budget constraints with the competing requirements of fleet readiness, reliability, and safety. Recently, considerable research is going on to develop an integrated Prognostic, and Health Management (PHM) [1, 2] system. Current aerospace industry practice follows a damage-tolerant reliability engineering model whereby structural components are regularly inspected and replaced. The replaced components are not necessarily at the end of its designed useful life. These practices unnecessarily add to the overhauling expenditure and time. The damage-tolerant

reliability designs are generally based on a physics-based fracture mechanics approach or a data driven stochastic approach. The physics-based damage tolerance approach that is widely practiced [3–6] and constantly been improved is primarily based on linear fracture mechanics, as far as fatigue failure is concerned. Another damage tolerance approach, known as a life usage model [7, 8], is also widely used and is based on gathering statistical information about how long a component endures before failure, and uses these statistics, collected from a large population sample, to make remaining life predictions for individual components. However, these predictions are not based on measured characteristics of the individual components. In addition, fatigue life of aircraft structural components under service loading conditions [9, 10] is often analyzed and predicted based on crack growth rates obtained from constant-amplitude fatigue testing data. In contrast to the fatigue crack growth due to constant amplitude loading, crack growth caused by variable amplitude loadings is characterized by retardation and acceleration effects [11], which extend or reduce the lifetime of structures. Currently there are many physics-based models [3–6, 12, 13] with empirical parameters available to model crack growth with retardation and acceleration effects. These models reasonably capture the dynamics of the fatigue crack growth under variable loading in a deterministic framework. However, these models do not explicitly model the uncertainty in crack growth that arises due to scatter [9, 10] in microstructural properties and subsequent uncertainty propagation due to loading sequence effects.

Current research works varying from medical [14] to aerospace applications [15] shows the effective use of neural network for diagnostic and prognostic systems. However, a few of these neural network models are based on the explicit uncertainty quantification approach, like the Bayesian uncertainty model. It is noted that Bayesian methods allow [16] complex neural network models to be used without fear of "over fitting" that can occur with traditional neural network learning methods. However, the Bayesian analysis of neural networks is difficult [17] because a simple prior over weighing parameters of the network requires a complex prior over underlying functions and, hence, it becomes computationally intractable. The present paper discusses the use of the Gaussian Process (GP) approach [17, 18] for a prognostic system that explicitly models Bayesian uncertainty into the predictive model. The GP model is a simplification of the Bayesian analysis of neural networks by assuming that the multivariate random variables are Gaussian random variables in an infinite (countable or continuous) index set. The Gaussian process model projects the input space to an output space by probabilistically inferring the underlying nonlinear function relating input and output.

In earlier work [19] we presented a GP offline model for fatigue life prediction under variable loading. In the mentioned work only four specimen data sets were considered. Compared to our earlier work, the present paper discusses both offline and online prediction models. In addition, the present paper discusses rate based prediction which better resembles to a fracture mechanics based crack growth prediction approach. Furthermore, unlike our previous work which, was based on only four specimens data the present model is based on 18 specimens test data. It is to be noted that; such a large test data under variable fatigue loading is hardly available in open literature. For the present offline prediction model the input space of the model is trained with parameters that affect fatigue crack growth such as, number of fatigue cycles, minimum load, maximum load, and load ratio. In turn, the output space is linked to the corresponding crack lengths or crack growth rates. The GP models the scatter in fatigue crack growth that arises due to microstructural variability, loading uncertainty, and variability due to manufacturing tolerance. Once the GP is trained with a known input-output data set, it can predict the output crack length or its rate under the particular loading envelope. For online prediction, the model input space is trained using features found from piezoelectric sensor signals rather than with loading parameters, whereas, the output space is trained with corresponding crack lengths.

Technical Approach

Gaussian Process Offline Predictive Model

The goal of the GP offline data driven prediction model is to compute the distribution of future damage states for which the damage affecting physical parameters are known, e.g., the loading or compliance change patterns, number of fatigue cycles elapsed, initial damage size, environmental condition, or grain size distributions. The GP assumes the scatter in crack growth (as schematically shown in Fig. 1) is due to the variation in these parameters. Due to the scatter in crack length or the damage state, at any instance, the damage state follows a distribution rather than being deterministic. GP assumes this individual distribution to be a Gaussian distribution with different mean and variance and evaluates the Bayesian conditional distribution of the future damage state (N+1$^{\text{th}}$ damage state depicted in Fig. 1) as $f\left(a_{N+1}\middle|D=\{\mathbf{x}_i,a_i\}_{i=1}^{N},\mathbf{x}_{N+1}\right)$, i.e., to compute the probability distribution of the damage state a_{N+1} given a test input $\mathbf{x}_{N+1}$ and a set of 'N' training points $D=\{\mathbf{x}_i,a_i\}_{i=1}^{N}$, where a_i is the i^{th} random variable at the i^{th} fatigue cycle.

Let us assume that the damage variable a_i at the i^{th} damage instances follows a Gaussian distribution. Following the

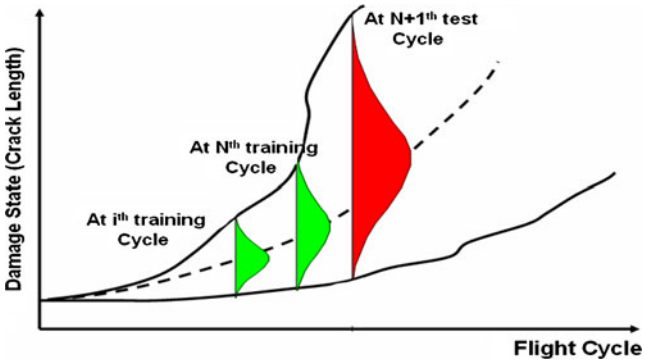

Fig. 1 Schematic of individual distributions at various instances of time those collectively make Gaussian Process

work of MacKay [16, 17] and Rasmussen and Williams [18] the Bayesian conditional distribution over a_{N+1} at N+1th damage instances can be given as

$$f\left(a_{N+1}|D,\mathbf{K}_N\left(\mathbf{x}_i,\mathbf{x}_j\right),\mathbf{x}_{N+1},\Theta\right) = \frac{1}{Z}\exp\left(-\frac{(a_{N+1}-\widehat{a}_{N+1})}{2\sigma^2_{\widehat{a}_{N+1}}}\right) \tag{1}$$

Where Z is an appropriate normalizing constant and the mean and variance of the new distribution are, given as

$$\widehat{a}_{N+1} = \mathbf{k}_{N+1}^T\mathbf{K}_N^{-1}\mathbf{a}_N \quad ; \tag{2}$$
$$\sigma^2_{\widehat{a}_{N+1}} = \kappa - \mathbf{k}_{N+1}^T\mathbf{K}_N^{-1}\mathbf{k}_{N+1}$$

Also to note that, equation (1) represent a zero-mean GP. To use equation (1), the training data set is first scaled such that it has a mean equal to zero. However, an appropriate offset equal to the mean of the original training data, has to be added to the predicted crack length. In equation (2) $\mathbf{a}_N$ is the $(N\times 1)$ training output vector which in this case it is the crack length or crack growth rate. Also κ, $\mathbf{k}_{N+1}$, $\mathbf{K}_N$ are the partitioned components of N+1th instances kernel matrix $\mathbf{K}_{N+1}$ and can respectively described as

$$\kappa = k(\mathbf{x}_{N+1},\mathbf{x}_{N+1}) \quad ; \quad k_i = k(\mathbf{x}_{N+1},\mathbf{x}_i)_{i=1,2,\cdots,N};$$
$$K_{i,j} = k\left(\mathbf{x}_i,\mathbf{x}_j\right)_{i,j=1,2,\cdots,N} \tag{3}$$

In equation (3) k is the assumed kernel function. There are many possible choices of prior kernel functions. From a modeling point of view, the objective is to specify a prior kernel that contains our assumptions about the structure or the process being modeled. Formally, a function that will generate a positive definite kernel matrix for any set of inputs is required. A non-stationary multi-layer perceptron kernel function [20] is used for the current GP model and is given by

$$k\left(\mathbf{x}_i,\mathbf{x}_j\right) = \Theta_1 Sin^{-1}\left(\frac{(\mathbf{x}_i)^T\Theta_2(\mathbf{x}_j)}{\sqrt{\left(1+(\mathbf{x}_i)^T\Theta_2(\mathbf{x}_i)\right)}\sqrt{\left(1+(\mathbf{x}_j)^T\Theta_2(\mathbf{x}_j)\right)}}\right)+\Theta_3 \tag{4}$$

For real world data these are generally scattered, thus it is assumed that the chosen kernel function will generate a positive definite kernel matrix. The parameters $\Theta = \{\Theta_1,\Theta_2,\Theta_3\}$ in equation (4) are unknowns and are estimated by minimizing the negative log likelihood function, given below

$$L = -\frac{1}{2}\log\det K_N - \frac{1}{2}\mathbf{a}_N^T\mathbf{K}_N^{-1}\mathbf{a}_N - \frac{N}{2}\log 2\Pi \tag{5}$$

The hyperparameters $\Theta = \{\Theta_1,\Theta_2,\Theta_3\}$ are initialized to reasonable values and then the conjugate gradient method is used to search for their optimal values. Initially, the kernel function given in equation (4) is evaluated using the assumed initial hyperparameters and the known input space vectors $\mathbf{x}_i$. The input space vectors $\mathbf{x}_i$ are a 'd' dimensional vector with the individual elements of the vector containing the value of the different fatigue affecting parameters at the i^{th} instance. Whereas, 'd' is the number of fatigue affecting physical parameters for the offline predictive model and is the dimension of the input space. For the present offline prediction model the input space vectors $\mathbf{x}_i$ of the model is trained with parameters that affect fatigue crack growth such as, number of fatigue cycles, minimum load, maximum load, and load ratio. In turn, the output space scalar a_i consists of either the corresponding crack length or the crack growth rate. Once the GP is trained with a known input-output data set, it can predict the output crack length or its rate under the particular loading envelope. The above discussed GP prediction approach for direct crack length prediction can be summarized as follows. Similar procedure can be followed for crack growth rate prediction.

Step-1 Arrange the training data in the following GP input-output form

$$\begin{bmatrix} U^{\max}_{p=1,q=1} & U^{\min}_{p=1,q=1} & R_{p=1,q=1} & n_{p=1,q=1} \\ U^{\max}_{p=1,q=2} & U^{\min}_{p=1,q=2} & R_{p=1,q=2} & n_{p=1,q=2} \\ \bullet & \bullet & \bullet & \bullet \\ U^{\max}_{p=1,q=N} & U^{\min}_{p=1,q=N} & R_{p=1,q=N} & n_{p=1,q=N_1} \\ \bullet & \bullet & \bullet & \bullet \\ U^{\max}_{p=P,q=N_P} & U^{\min}_{p=P,q=N_P} & R_{p=P,q=N_P} & n_{p=P,q=N_P} \end{bmatrix} \rightarrow \begin{bmatrix} a_{p=1,q=1} \\ a_{p=1,q=2} \\ \bullet \\ a_{p=1,q=N_1} \\ \bullet \\ a_{p=P,q=N_P} \end{bmatrix} \tag{6}$$

The left hand side matrix of the above expression represents the input space, whereas the right hand side vector represents the output space. Also,

$U^{\max}_{p,q}$, $U^{\min}_{p,q}$, $R^{\max}_{p,q}$, $n_{p,q}$ and $a_{p,q}$ represent the maximum load, minimum load, load ratio, number of fatigue cycle and crack length, respectively. The subscript p and q represent the specimen number and the corresponding fatigue cycles, respectively.

Step-2 Logarithmically scale both the input matrix and output vector of the training data given in equation (6). In addition, to follow a zero mean GP as described by equation (1), the output crack lengths have to be scaled as zero mean data.

Step-3 Using equation (4), evaluate the kernel matrix, where $\mathbf{x}_i$ and $\mathbf{x}_j$ represent the two adjacent rows of the input matrix given in equation (6). It is to be noted that the hyperparameters $\Theta = \{\Theta_1, \Theta_2, \Theta_3\}$ in the kernel matrix are unknown.

Step-4 Iteratively minimize the negative log-likelihood function given in equation (5) to estimate the unknown hyperparameters $\Theta = \{\Theta_1, \Theta_2, \Theta_3\}$.

Step-5 Use the estimated hyperparameters $\Theta = \{\Theta_1, \Theta_2, \Theta_3\}$ and known inputs to evaluate the new kernel matrix for test specimen. The new kernel matrix has to be evaluated using the input matrix that includes input vectors $\mathbf{x}_i$ of both training and test cases. The combined input-output relation for the training and test case is given as below.

$$\begin{bmatrix} U^{\max}_{p=1,q=1} & U^{\min}_{p=1,q=1} & R_{p=1,q=1} & n_{p=1,q=1} \\ U^{\max}_{p=1,q=2} & U^{\min}_{p=1,q=2} & R_{p=1,q=2} & n_{p=1,q=2} \\ \bullet & \bullet & \bullet & \bullet \\ U^{\max}_{p=1,q=N_1} & U^{\min}_{p=1,q=N_1} & R_{p=1,q=N_1} & n_{p=1,q=N_1} \\ \bullet & \bullet & \bullet & \bullet \\ U^{\max}_{p=P,q=N_P} & U^{\min}_{p=P,q=N_P} & R_{p=P,q=N_P} & n_{p=P,q=N_P} \\ U^{\max}_{t=1,q=N_1} & U^{\min}_{t=1,q=N_1} & R_{t=1,q=N_1} & n_{t=1,q=N_1} \\ \bullet & \bullet & \bullet & \bullet \\ U^{\max}_{t=T,q=N_T} & U^{\min}_{t=T,q=N_T} & R_{t=T,q=N_T} & n_{t=T,q=N_T} \end{bmatrix} \rightarrow \begin{bmatrix} a_{p=1,q=1} \\ a_{p=1,q=2} \\ \bullet \\ a_{p=1,q=N_1} \\ \bullet \\ a_{p=P,q=N_P} \\ ? \\ ? \\ ? \end{bmatrix} \tag{7}$$

In equation (7), the subscript 't' represents the test specimen number and the question mark "?" represents unknown crack length to be evaluated using equation (2). The estimated crack length has to be adequately scaled back to compensate for the scaling performed in step-2.

Gaussian Process Based Online Predictive Model

General architecture of Gaussian process online model

In the previous section the offline prediction with a Gaussian process input space generated from loading change information and other fatigue affecting parameters was discussed. However, in real time it is hardly possible to measure loading or compliance change information in a full scale component. However, small piezoelectric sensors in the full scale hardware can be mounted to measure equivalent damage state information in a real time situation. These sensor signals can be obtained at regular instances and after necessary signal processing, it can be fed to the GP input space to map the output space crack length or crack growth rate. Once the training input space and training output space are formed using equations (1–7), the new predicted mean and variance for a new test input space can be predicted. A general architecture for the online prediction model is shown in Fig. 2. The figure shows the multiple sensor signals that are collected at different instances of a fatigue loading envelope. These signals form the signal space for the feature extraction algorithms, such as Principal Component Analysis (PCA). The feature extraction algorithm statistically denoises the original signal and generates ranked feature vectors ordered according to its information content. Once the feature vector is found, it can fed to the GP input space to map the original sensor signal with the corresponding crack length or crack growth rate. The details of the feature extraction algorithms are discussed in the following subsection.

Principal Component Analysis (PCA)

Principal component analysis [21, 22] is an orthogonal basis transformation that has been widely used for multivariate data analysis and dimensionality reduction. Intuitively, PCA is a process that identifies the direction of the principal components where the variance of changes in dynamics is a maximum. Assuming 'M' different observations and each observation with d dimensions (as described in Fig. 2), the input signal space $\mathbf{y}_p$ is a $M \times d$ matrix. It is noted that each sensor observation is a $1 \times d$ vector expressed as $\mathbf{y}_d$. Then the centered $d \times d$ covariance matrix of the data set can be found as

$$\mathbf{C}_d = \left\langle \left(\mathbf{y}_q - \left\langle \mathbf{y}_p \right\rangle\right)\left(\mathbf{y}_q - \left\langle \mathbf{y}_p \right\rangle\right)^T \right\rangle \tag{8}$$

Then the covariance matrix is diagonalized to obtain the principal components and the diagonalization can be performed by solving the following eigenvalue problem:

$$\lambda v = C_d v \tag{9}$$

The coordinates in the eigenvector basis are called principal components. The magnitude of an eigenvalue λ corresponding to an eigenvector v of covariance matrix $\mathbf{C}_d$ equals the amount of variance in the direction of v. Furthermore, the direction of the first 'n' eigenvectors corresponding to the largest 'n' eigenvalues covers as much variance as possible by 'n' orthogonal directions. For the present online prediction

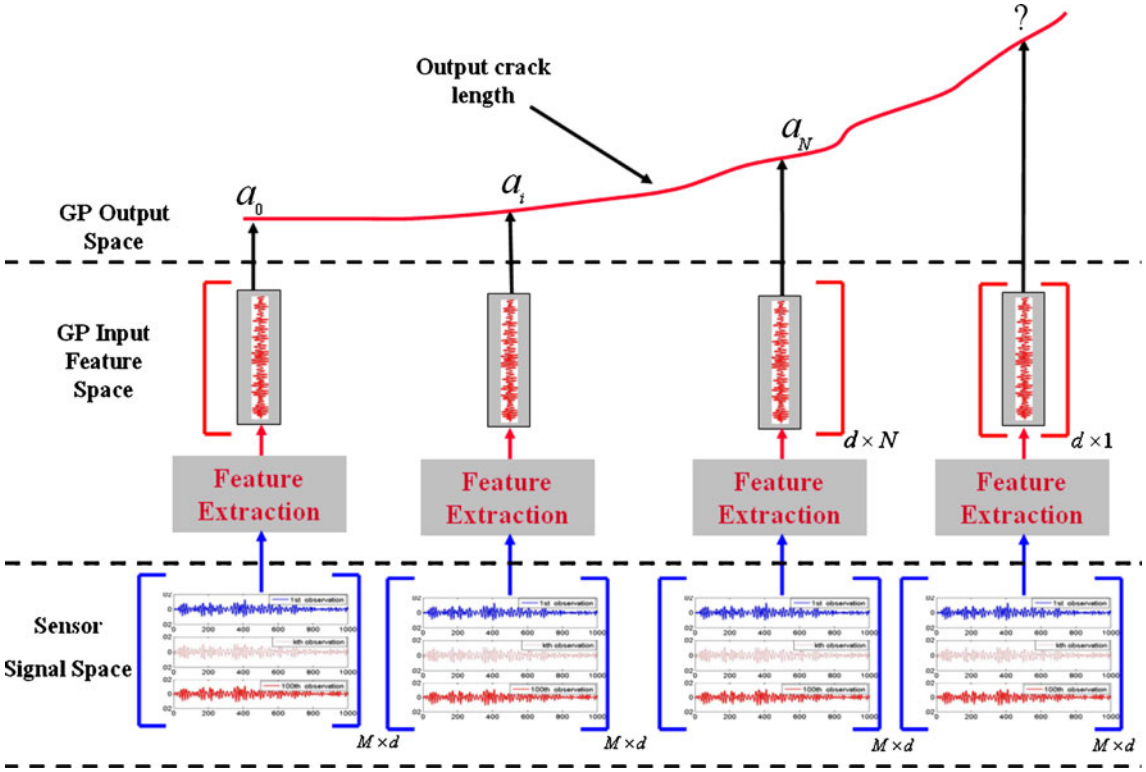

Fig. 2 General architecture for online predictive model

problem the first eigenvector is considered to be the most pristine quantity with maximum buried information and thus called the principal feature vector. This $d \times 1$ principal feature vector is used to construct the i^{th} instance input vector $\mathbf{x}_i$ (ref. Fig. 2) of the GP online model. The corresponding i^{th} instance output scalar a_i corresponds either to known (for the training case) or unknown (for the test case) crack length or crack growth rate.

Numerical Verification

Numerical studies have been conducted to verify the effectiveness of the GP model discussed in the previous section. The details of the experiment and numerical studies are discussed below.

Fatigue Test Experiment

The fatigue experiments were performed using an Instron 1331 servo-hydraulic load frame operating at 20 Hz. Eighteen Al 2024 T351 Compact Tension (CT) samples, each 6.31 mm thick, were tested. These specimens were fabricated according to ASTM E647-93 with an average width of 25.53 mm (from the center of the pin hole to the edge of the specimen) and an average height of 30.6 mm. To simulate typical flight loading conditions a variable load spectrum was programmed into the digital controller of the load frame. The spectrum, as coded to the load-cell, is shown in Fig. 3. However, due to noise and compliance effects, the load that was actually applied to the CT specimens were somewhat different than that programmed to the controller. The minimum and maximum loads applied to the specimens were measured through the load cell and are used to construct the GP input space. It must be noted that for each sample the frame was stopped and the corresponding load cell outputs were recorded at random instances during the experiment. Each time the test was stopped, a high resolution picture of the cracked sample was taken using a digital camera to generate the output space crack length data. The corresponding measured crack lengths for different samples are depicted in Fig. 4. It is noted that CT samples are named from ct416a to ct436a.

The prefix ‘ct’ symbolizes compact tension, the middle number shows the number of the sample, and the suffix ‘a’ indicates that the initial notch is made along the rolling direction of the aluminum plate. The absence of some numbers, such as ct422a (ref. Fig. 4) imply that the data could not be collected for those samples due to premature failure of the specimen (due to faulty handling of fatigue frame). Out of a total of 18 samples for which the fatigue crack length data were available, four samples: ct417a,

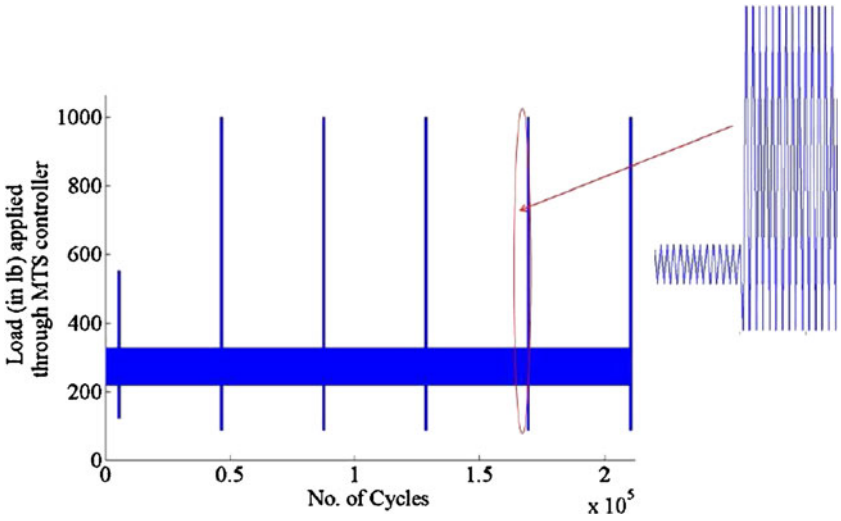

Fig. 3 Loading spectrum programmed to load frame controller

ct419a, ct421a and ct423a were instrumented with a piezoelectric sensor and an actuator. A typical instrumented sample after the fatigue test is shown in Fig. 5. When the test frame was stopped, the piezoelectric actuator was excited with a narrow band burst signal. The corresponding sensor signal was collected using a National Instrument (NI) data acquisition system. These collected signals are used as input to the online predictive model, which will be discussed in detail in subsequent section. The CT specimens were not removed from the test frame and were kept under loading conditions while collecting sensor data to simulate realistic on-board conditions. At each stopping instant, 150 sensor observations were collected, out of which 100 were selected based on a Fast Fourier Transform filter. These 100 observations were used as inputs to PCA for feature extraction at those instances.

Gaussian Process Offline Prediction

The GP input spaces are constructed using the load cell readings at different instances and the fatigue cycles at those instances. It is noted that the load cell reading changes at different fatigue instances because of the compliance change of the specimen. The individual $\mathbf{x}_i$ is a $d\times 1$ vector with elements comprising fatigue cycles, minimum load, maximum load and load ratio. The individual $\mathbf{x}_i$ form the $d\times N$ input training space and the corresponding $1\times N$ observed crack lengths (from high resolution images) form the training output space. The dimension of the input space can be varied to any number, but for the present study it is restricted to one for single variate predictions and four for multivariate predictions. For a new test instance with known input $\mathbf{x}_i$ the corresponding

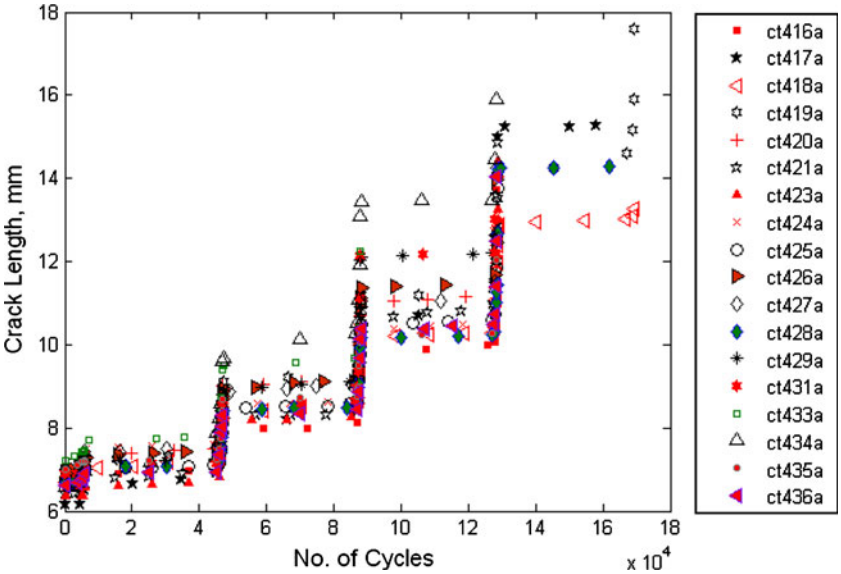

Fig. 4 Experimental crack length data

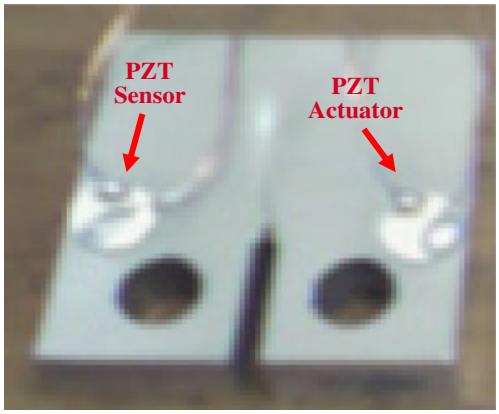

Fig. 5 Instrumented CT specimen

mean output crack length is predicted using equation (2). Before using the data for GP prediction the input and output space variables are logarithmically scaled. In addition to follow a zero mean Gaussian process as described in equation (1), the output crack lengths are scaled as zero mean random data. Both the single and multivariate predictions of output crack lengths are made for all 18 CT specimen (Fig. 6). It is noted that while selecting a particular sample as a test specimen, the data collected from the other 17 samples are used for training the GP model. Figures 6(a, b) show the singlevariate and multivariate GP predictions of crack length, respectively. Comparing Figs. 4, 6(a), it can be seen that even though the singlevariate GP, with time (number of cycles) as the only input variable, is able to predict an average crack growth curve, it is unable to track the transient jump in crack growth that arises due to transient over-load cycles (Fig. 3). The only exception is sample ct419a where a good prediction is observed [Fig. 6(a)]. However, comparing Figs. 4, 6(b) it can be seen that the multivariate GP captures those transient loading effects for most of the samples. To further improve the GP offline prediction, a rate-based prediction has been performed. In this case, rather than directly predicting the crack length, the crack growth rate is predicted first and then it is integrated with respect to time, to estimate the corresponding crack length. From a numerical perspective, it is better to predict the derivative than to predict an integral (crack length in this case) for a highly non-smooth function. Also, from a fracture mechanics perspective, fatigue crack growth is normally expressed in terms of a first order nonlinear rate equation. Therefore, although the direct crack length GP model is capable of capturing the nonlinearity, the rate prediction allows capturing first order crack growth rate and capturing the physics of a dynamic system. However, it must be noted that to perform a rate based crack growth estimation, the cycle by cycle rate has to be integrated for the most correct crack growth curve estimation. In the present case, where experimental data were available only at those discrete instances, the crack growth rate prediction is possible. Nevertheless, to estimate a continuous crack length when the crack growth rate is not available at any cycle, the crack growth rate for the previous cycle is assumed for the current cycle. A comparison of GP prediction of crack growth rate and the crack growth rate observed from experiments can be seen in Fig. 7(a, b). The figures show that with the exception of a slightly lower rate prediction compared to the experimental rate, there is a good correlation between predicted and observed rates within the context of transient overloading. The slight under prediction in rate compared to experimental values is attributed to the lack of continuous experimental data, which led to the use of an averaging technique for rate estimation over large numbers

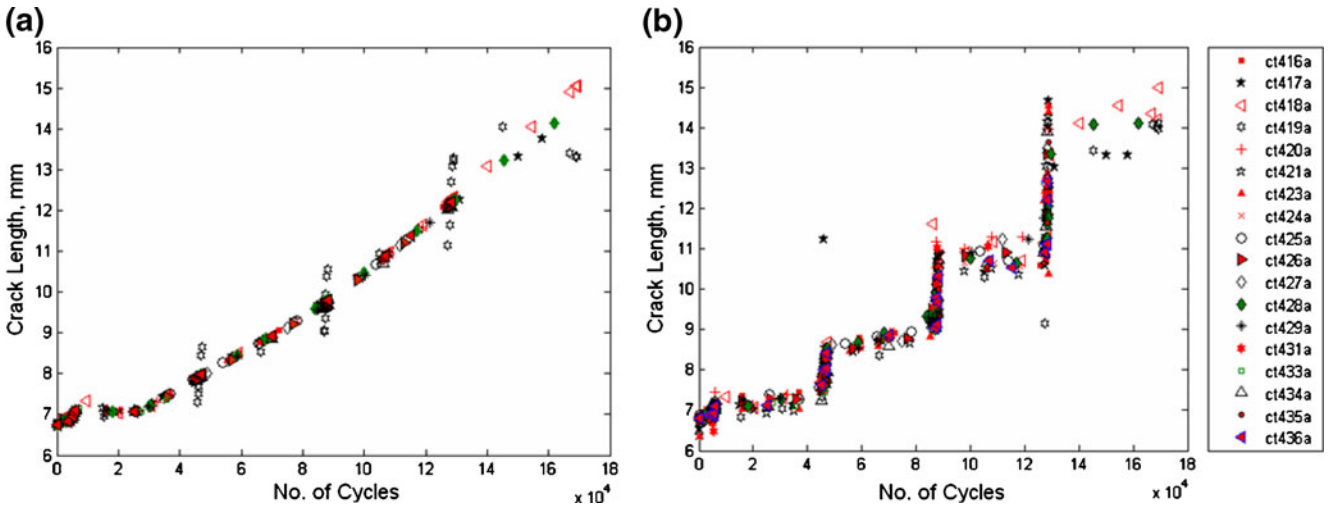

Fig. 6 (**a**) Single variate prediction. (**b**) Multi variate prediction

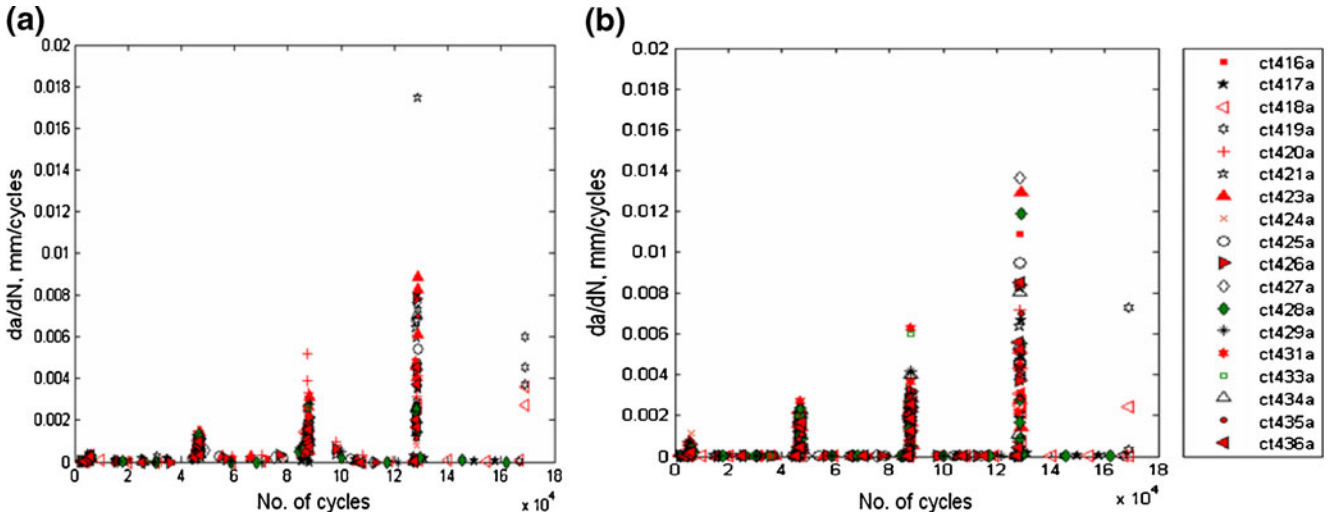

Fig. 7 (**a**) Predicted rate from multivariate GP. (**b**) Rate from experimental observation

of cycles. Figure 8(a) shows the continuous crack length estimated for different samples and Fig. 8(b) shows the crack lengths at discrete instances (where experimental data were collected). Comparing Figs. 4, 8(b), it is found that the prediction accuracy improves compared to estimating crack length directly as shown in Fig. 6(b).

Gaussian Process Online Prediction

For the online GP prediction the input vector $\mathbf{x}_i$ in equation (4) is fed with sensor signal features found using PCA. At each observation, the piezoelectric actuator is actuated with a narrow band burst signal. The burst signal, as shown in Fig. 9, has a central frequency of 135 KHz and a sampling frequency of 2 MS/sec. For each actuation, 150 sensor observations are obtained to have a probabilistic feature extraction. Out of the 150 sensor observations only 100 are chosen for the feature extraction. At any typical fatigue instance the representative sensor signals used for feature extraction are depicted in Fig. 10. These 100 observations are selected based on a Fast Fourier Transform filter that allows selecting a particular sensor signal with a central frequency in the range of 135± 30 KHz. The selection of the 30 KHz upper and lower limit is based on the assumption that the maximum frequency variation of the observed signal will not cross these limits over the fatigue loading envelope. The above selected frequency band ensures that signals containing

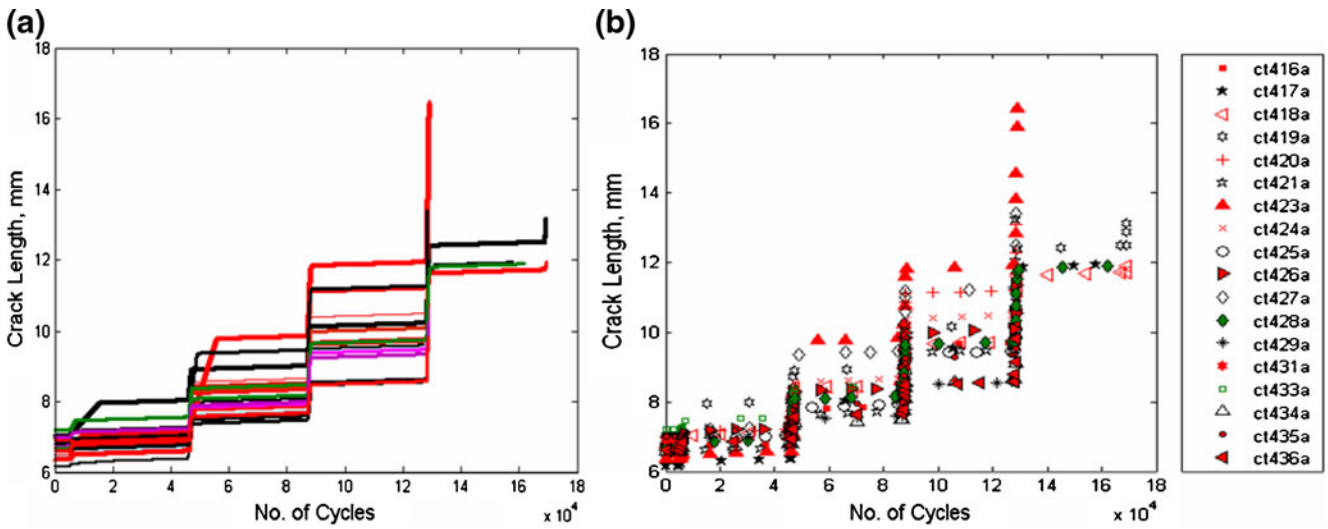

Fig. 8 Continuous crack length from integration of GP estimated rate (**b**) Discrete crack lengths (at experimental stopping instances) captured from (**a**)

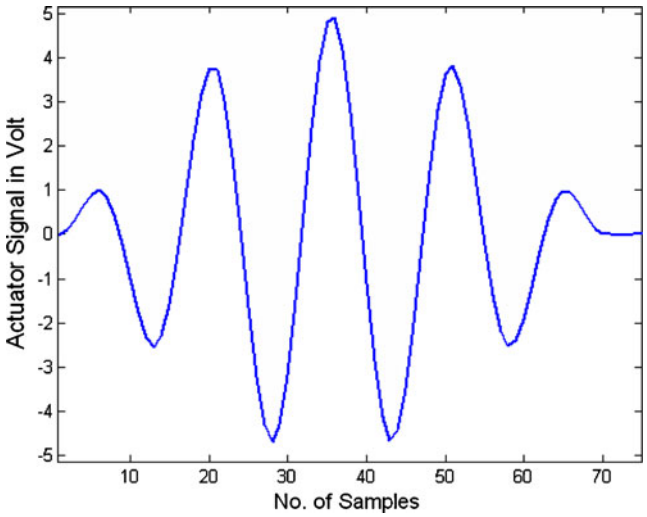

Fig. 9 Burst signal applied through PZT actuator

low frequency noise (due to the hydraulic pump of the fatigue frame) or high frequency noise (due to other environmental factors) are not selected in the feature extraction process. Once the first 100 sensor signals (each of 1000 samples) are selected, those signals are used as input in the feature extraction algorithm. With this information, the value of 'M' and 'd' in the expression $\left\{\mathbf{y}_p \in R^M | p = 1, 2, \cdots d\right\}$ becomes M=100 and d=1000. The reason for selecting 100 similar observations for feature extraction is to statistically select the best features from the original signal, which may have environmental noise within the frequency range of 135±30 KHz. Using the above mentioned signals, the covariance matrix (equation 8) for PCA is evaluated. The covariance matrix for PCA at a typical observation instance is shown in Fig. 11. The covariance matrix is used to solve the eigenvalue problem described in equation (9) for PCA feature extraction. From the eigenvalue analysis the first

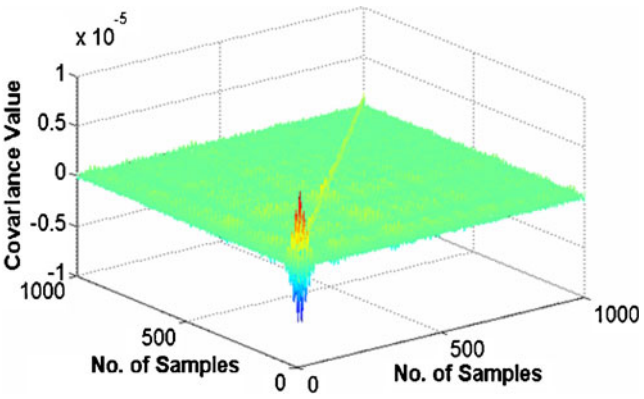

Fig. 11 Covariance at a typical fatigue instance

eigenvector is selected as the feature vector. It must be noted that the feature extraction is done at each discrete instance when the fatigue frame was stopped to collect data. This leads to 'N' (equations 1–7) number of feature vectors, each of length d=1000. The first feature vector at a typical fatigue instance is shown in Fig. 12. Once the feature vectors are obtained for different instances, the GP input and output spaces are formed. The input training space of size $d \times N$ is formed from the 'N' feature vectors. The corresponding training output space consists of $1 \times N$ observed crack length vector, which is used in the offline prediction. Once the GP training input and output spaces are formed the prediction of an unseen output state, here the crack length or crack growth rate, is made using equations (1–7). It is noted that, for the online prediction the input space is not scaled, whereas the output space is scaled with zero mean, unit variance scaling. This type of scaling is performed to ensure that both the input and the output spaces have similar variances, though not necessarily the same. It is noted that the GP works well when the distribution of the underlying variables have similar mean and variances.

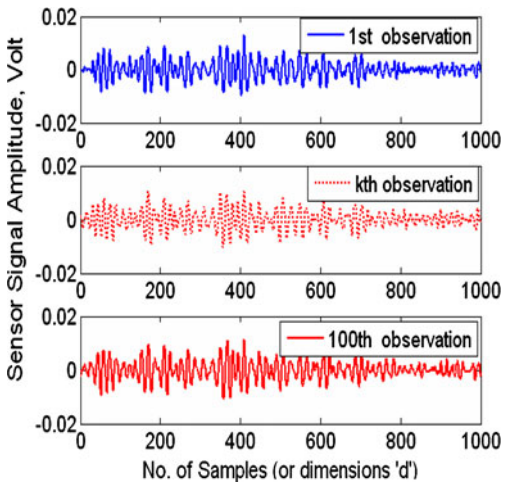

Fig. 10 Representative sensor signal for feature extraction

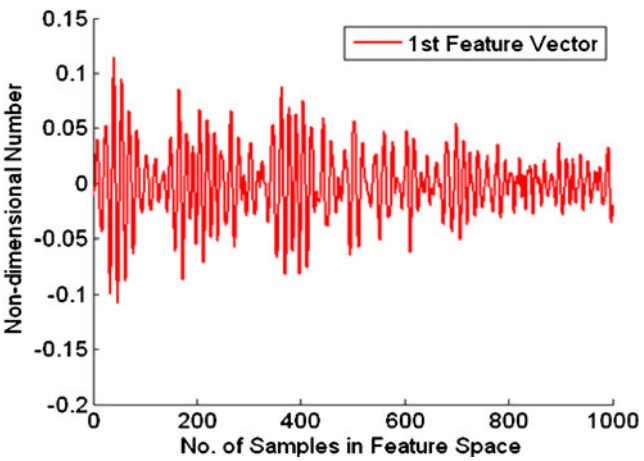

Fig. 12 First feature vector from PCA

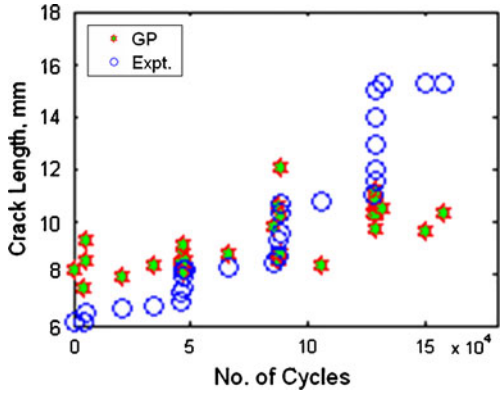

Fig. 13 Direct crack length predictions for ct417a specimen

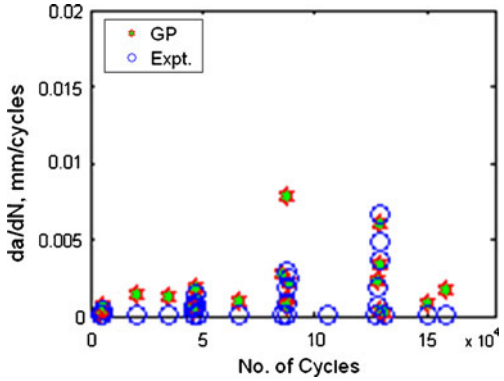

Fig. 14 Crack growth rate predictions for ct417a specimen

The direct crack growth prediction using PCA feature extraction technique is shown in Fig. 13. It is noted that piezoelectric sensor data were available only for four specimens (ct417a, ct419a, ct421a and ct423a). Therefore, unlike the offline model for which data from 18 specimens were available, for the online model three specimen data are used to train the GP and the data from the fourth one is used for testing. For the present study, data from ct417a is used as the test specimen and ct419a, ct421a and ct423a are considered as training specimens. Figure 13 shows the predicted and actual crack lengths for ct417a specimen. This figure indicates that the correlation between experiment and prediction is not as good for the entire fatigue loading envelope as seen for the offline prediction. However, there is a similar qualitative trend between experiment and prediction, particularly during the transient high load regime. This correlation is because during the transient over-load regime larger numbers of data points are available (refer Fig. 4) compared to the lower load regime. During the lower load regime, the crack growth is assumed stable and hence fewer data points are collected over this regime. In addition, the crack growth rate magnitude during the lower load regime is approximately one and half times less compared to the average crack growth rate during the transient high load regime. For example, for the ct423a sample (ref. Fig. 7), the average crack growth rate during the lower load regime is approximately 1.041×10^{-5} mm/cycles, whereas the approximate average rate during the third high load regime (87e3–88e3 cycles) is 1.4×10^{-4} mm/cycles. Crack growth rates are also predicted using the GP online predictive model. The crack growth rates are predicted using PCA based feature extraction techniques and shown in Fig. 14.

The figures indicate that unlike the case of direct crack growth prediction, there is a better correlation between experimental and predicted rates. Once the crack growth rates are predicted using GP, the continuous crack length can be estimated via cycle by cycle integration of the predicted rates. In the absence of rate information at any particular cycle, a strategy similar to that for the offline prediction is employed to estimate the corresponding crack length. However, it is noted that for the online prediction case, while estimating the crack length in the lower load regime, the integration algorithm is modified to select the minimum between the GP predicted rate and the value of 1.041×10^{-5} mm/cycles. This value is found from experimental observations in the lower load regime of CT423a specimen, but it is a representative value from the other specimens. The purpose of using this value in the integration process is to avoid using a spurious rate as predicted from the GP particularly at the lower load regime. The continuous crack lengths calculated from the predicted rate are shown in Fig. 15. It is seen that the rate based prediction of crack growth has better correlation with experiments compared to the direct GP prediction of crack growth as shown in Fig. 13.

Conclusion

Offline and online data driven models are proposed for fatigue crack growth prediction. The proposed Bayesian

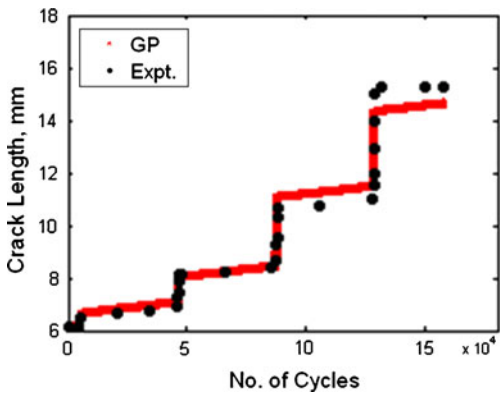

Fig. 15 Estimated continuous crack lengths for ct417a specimen using linear integration and using predicted crack growth rates shown in Fig. 14

based GP approach predicts the fatigue crack of Al 2024 CT specimens under variable loading. The input space of the model is trained with parameters such as number of fatigue cycles, minimum load, maximum load, and load ratio for the offline prediction. The input space is trained using features obtained from piezoelectric sensor signals for the online prediction. In both offline and online cases, the output space is trained with known associated crack lengths. Using the trained GP model, predictions are made for the unknown output space (crack length or crack growth rate) and the results are validated with experiments. The numerical results indicate that the multivariate offline prediction model outperforms the single variate prediction model. In addition, it is found that the rate based crack growth prediction has better correlation with actual values compared to the direct crack growth prediction. Similar trend is also observed for online prediction using piezoelectric sensor signal features.

Acknowledgments This research was supported by the MURI Program, Air Force Office of Scientific Research, grant number: FA9550-06-1-0309; Technical Monitor, Dr. David S Stargel.

References

1. Hess A, Calvello G, Frith P, Engel SJ, Hoitsma D (2006) Challenges, issues, and lessons learned chasing the "Big P": real predictive prognostics Part 2. Proceedings of IEEE Aerospace Conference, AERO20061656124 4–11:1–19
2. Hess A, Frith P (2002) The Joint Strike Fighter (JSF) PHM concept: potential impact on aging aircraft problems. Proceedings of IEEE Aerospace Conference, AERO20021036144 6:6-3021–6-3026
3. Newman JC Jr (1982) Prediction of fatigue crack growth under variable-amplitude and spectrum loading using a closure model. ASTM STP 761:255–277
4. Newman JC Jr (1984) A crack-opening stress equation for fatigue crack growth. Int J Fract 24:R131–R135
5. Newman JC Jr (1992) FASTRAN-II—A fatigue crack growth structural analysis program. Langley Research Center, NASA TM 104159
6. Harter JA (1999) AFGROW users' guide and technical manual. Air force Research Laboratory, AFRL-VA-WP-1999-3016
7. Miner MA (1945) Cumulative damage in fatigue. Journal of Applied Mechanics A-159–A-164
8. Samborsky DD, Wilson TJ, Mandell JF (2007) Comparison of tensile fatigue resistance and constant life diagrams for several potential wind turbine blade laminates. *Proceedings of Wind Energy Symposium*, Reno, Nevada
9. Zapateroa J, Domnguez J (1990) A statistical approach to fatigue life predictions under random loading. Int J Fatigue 12(2):107–114
10. Yongming L, Sankaran M (2007) Stochastic fatigue damage modeling under variable amplitude loading. Int J Fatigue 29 (6):1149–1161
11. Elber W (1970) Fatigue crack closure under cyclic tension. Eng Fract Mech 2:37–45
12. Ray A, Patankar RP (2001) Fatigue crack growth under variable amplitude loading—Part-I: model formulation in state-space setting. Appl Math Model J 25(11):979–994
13. Ray A, Patankar RP (2001) Fatigue crack growth under variable amplitude Loading—Part-II: code development and model validation. Appl Math Model J 25(11):995–1013
14. Ioannis A, Ilias M (2006) Neural network-based diagnostic and prognostic estimations in breast cancer microscopic instances. Med Biol Eng Comput 44(9):773–784
15. Vachtsevanos G, Wang P (2001) Fault prognosis using dynamic wavelet neural networks. Proceedings of IEEE Systems Readiness Technology Conference, AUTEST.2001.949467, pp 857–870
16. MacKay DJC (1992) Bayesian interpolation. Neural Comput 4 (3):415–447
17. MacKay DJC (1998) Introduction to Gaussian processes. In: Bishop CM (ed) Neural networks and machine learning, vol 168. NATO ASI Series, Springer, Berlin, pp 133–165
18. Rasmussen C, Williams C (2006) Gaussian processes for machine learning. MIT Press, Cambridge, MA
19. Mohanty S, Das S, Chattopadhyay A, Peralta P (2009) Gaussian process time series model for life prognosis of metallic structure. J Intell Mater Syst Struct 20(8):887–896
20. Williams CKI (1997) Computing with infinite networks. In: Mozer MC, Jordan MI, Petsche T (eds) Advances in neural information processing systems, vol 9. MIT Press, Cambridge, MA
21. Smith L. A tutorial on principal component analysis. [online database], URL: http://www.cs.otago.ac.nz/cosc453/student_tutorials/principal_components.pdf, [cited 2002]
22. Rao CR (1964) The use and interpretation of principal component analysis in applied research. Sankhya A 26:329–358